

**A new calpain inhibitor protects left ventricular dysfunction induced by mild ischemia-reperfusion in *in situ* rat hearts**

D Takeshita<sup>1,a</sup>, M Tanaka<sup>1,4,a</sup>, S Mitsuyama<sup>1</sup>, Y Yoshikawa<sup>3</sup>, G-X Zhang<sup>1,2</sup>, K Obata<sup>1</sup>, H Ito<sup>1</sup>,  
S Taniguchi<sup>3</sup>, M Takaki<sup>1</sup>

<sup>1</sup>) Department of Physiology II, Nara Medical University

<sup>2</sup>) Department of Physiology, Medical College of Soochow University, Dushu Lake Campus,  
Suzhou Industrial Park, Suzhou 215123, P.R. China

<sup>3</sup>) Department of Thoracic and Cardiovascular Surgery, Nara Medical University

<sup>4</sup>) Faculty of Health Care Science, Himeji Dokkyo University

<sup>a</sup>These authors contributed equally to this work.

Author Contributions:

Miyako Takaki designed and supervised the present study. Daisuke Takeshita, Midori Tanaka, Shinichi Mitsuyama, Guo-Xing Zhang, Koji Obata, Haruo Ito and Miyako Takaki conducted experiments and obtained the data. Yoshiro Yoshikawa and Shigeki Taniguchi supervised the present study. Daisuke Takeshita and Miyako Takaki performed the data analysis and drafted the manuscript.

Running title: Calpain inhibition and exercise

Corresponding author:

Prof. Miyako Takaki, Ph.D.

Department of Physiology II, Nara Medical University School of Medicine

840 Shijo-cho, Kashihara, Nara 634-8521, Japan

Fax: +81-744-23-4696, Tel: +81-744-29-8829, Email: mtakaki@naramed-u.ac.jp

**Abstract**

We have previously indicated that a new soluble calpain inhibitor, SNJ-1945 (SNJ) attenuates cardiac dysfunction after cardioplegia arrest-reperfusion by inhibiting the proteolysis of  $\alpha$ -fodrin in *in vitro* study. Nevertheless, the *in vivo* study design is indispensable to explore realistic therapeutic approaches for clinical use. The aim of the present *in situ* study was to investigate whether SNJ attenuated left ventricular (LV) dysfunction (stunning) after mild ischemic-reperfusion (mI-R) in rat hearts. SNJ (60  $\mu$ mol/L, 5 ml i.p.) was injected 30 min before gradual and partial coronary occlusion at proximal left anterior descending artery. To investigate LV function, we obtained curvilinear end-systolic pressure-volume relation by increasing afterload 60 min after reperfusion. In mI-R group, specific LV functional indices at midrange LV volume ( $mLVV$ ), end-systolic pressure ( $ESP_{mLVV}$ ) and pressure-volume area ( $PVA_{mLVV}$ : a total mechanical energy per beat, linearly related to oxygen consumption) significantly decreased, but SNJ reversed these decreases to time control level. Furthermore, SNJ prevented the  $\alpha$ -fodrin degradation and attenuated degradation of  $Ca^{2+}$  handling proteins after mI-R. Our results indicate that improvements in LV function following mI-R injury are associated with inhibition of the proteolysis of  $\alpha$ -fodrin in *in situ* rat hearts. In conclusion, SNJ would be a promising tool to protect the heart from the stunning.

**Key words:** mild ischemic-reperfusion injury; cardioprotection;  $\alpha$ -fodrin; SNJ-1945; treadmill

**Abbreviations:** I-R, ischemic-reperfusion; NCX,  $Na^+$ - $Ca^{2+}$  exchanger; LV, left ventricular; mI-R, mild ischemic-reperfusion; LVV, left ventricular volume; LVP, left ventricular pressure; P-V, pressure-volume; ESP, end-systolic pressure; SV, stroke

volume;  $ESP_{ESV}$ , end-systolic pressure at end-systolic volume;  $E_a$ , arterial effective elastance; E-C, excitation-contraction; mLVV, midrange LVV;  $ESP_{mLVV}$ , end-systolic pressure at mLVV;  $PVA_{mLVV}$ , systolic pressure-volume area at mLVV; ESPVR, end-systolic pressure-volume relation; LTCC, L-type  $Ca^{2+}$  channel; SERCA2a, sarcoplasmic reticulum  $Ca^{2+}$  ATPase; ESV, end-systolic volume, EDV, end-diastolic volume; EF, ejection fraction; LVW, LV weight; BW, body weight; HR, heart rate.

## **Introduction**

It is well known that one of underlying mechanisms for ischemic-reperfusion (I-R) injury is  $\text{Ca}^{2+}$  overload resulting from increased  $\text{Ca}^{2+}$  influx mediated via reverse-mode  $\text{Na}^+$ - $\text{Ca}^{2+}$  exchanger (NCX)[1-4]. We have previously reported that reperfusion injury after KCl cardioplegic cardiac arrest leads to  $\text{Ca}^{2+}$  overload and the resultant left ventricular (LV) dysfunction similar to I-R injury [5]. The mechanisms of  $\text{Ca}^{2+}$  overload in this model are likely accumulation of intracellular  $\text{Na}^+$  and subsequent activation of reverse-mode NCX activity [6]. However, previous studies in our laboratory suggest that proteolysis of the cytoskeletal protein  $\alpha$ -fodrin by calpains may also play a role on LV dysfunction [5, 7, 8].

Calpain inhibition was found to prevent against the proteolysis of  $\alpha$ -fodrin due to reperfusion injury after global ischemia [8] and after KCl cardioplegic cardiac arrest [9]. It has been proposed that  $\alpha$ -fodrin maintains the integrity of the plasma membranes as a constituent of the membrane skeleton [10, 11]. Therefore, it seems likely that the degradation of  $\alpha$ -fodrin in membrane fractions would alter the properties of ion channels [12]. Indeed, the possibility that disruption of cytoskeletal proteins inactivates L-type  $\text{Ca}^{2+}$  channels has been reported [13].

Recently, we have reported that a novel calpain inhibitor, ((1S)-1((((1S)-1-benzyl-3-cyclopropyl-amino-2,3-di-oxopropyl) amino) carbonyl)-3-methylbutyl) carbamic acid 5-methoxy-3oxapentyl ester (SNJ-1945; SNJ) attenuates left ventricular (LV) dysfunction induced by reperfusion-injury after cardioplegic cardiac arrest, by inhibiting the proteolysis of  $\alpha$ -fodrin, without any effects on protein levels of sarcoplasmic reticulum  $\text{Ca}^{2+}$  ATPase (SERCA2a) and L-type  $\text{Ca}^{2+}$  channel (LTCC)[9]. This novel calpain inhibitor (SNJ) has been shown to have good aqueous solubility, good plasma

exposure, and good tissue penetration in rats and monkeys [14, 15]. Intraperitoneal administration of SNJ (160 mg/kg) for 14 days produced no obvious toxicity or abnormalities in rats [14]. Furthermore, it was reported that SNJ was effective against cerebral ischemia-induced damage [16], but there have been no reports on its efficacy against cardiac I-R injury in *in situ* hearts. Only our recent study reported that SNJ was effective against reperfusion injury after cardioplegic cardiac arrest, though in *in vitro* hearts [9].

Accordingly, the *in vivo* study design is indispensable to explore realistic therapeutic approaches for clinical use, since *in vivo* cardiac hemodynamics is regulated by autonomic nervous system and endocrine gland. These regulations are lacking in *in vitro* hearts. The aim of the present study was to investigate the cardioprotective effects of SNJ against mild I-R (mI-R) induced injury after gradual and partial coronary occlusion at proximal left anterior descending artery in rat *in situ* hearts using analysis of LV mechanical work.

## **METHODS**

The investigation conformed with the *Guide for the Care and Use of Laboratory Animals* published by the US National Institutes of Health (NIH Publication No. 85-23, revised 1996), and reviewed and approved by the animal care and use committee of Nara Medical University.

### ***Surgical preparation***

The trachea was intubated, and the rat was ventilated with room air under pentobarbital (50 mg/kg, i.p.) anesthesia. Body temperature was maintained normal using the warming plate. The chest was opened, and a conductance catheter (1.5 Fr)

[17] was introduced into the LV through an apical stab to obtain reliable LV volume (LVV) signal. A 1.5-Fr pressure catheter was also inserted through the apex into the LV to obtain reliable LV pressure (LVP) signal. Anesthetic level was sustained with pentobarbital intravenous infusion at  $0.5 \text{ mg kg}^{-1} \text{ h}^{-1}$  throughout the experiment.

#### ***Mild ischemic-reperfusion heart preparation***

Coronary gradual and partial occlusion was performed in 10 seconds by ligation of proximal left anterior descending artery and attached 1-mm diameter soft tube using bulldog clamp at the knot of suture (Figure 1A) under monitoring LV pressure-volume (P-V) loop. During this occlusion, P-V loop moderately shifted rightward and each stroke volume gradually decreased accompanied with increases in heart rate, but end-systolic pressure (ESP) hardly changed (Figure 1B). The survived rats did not cause lethal arrhythmia because of adequate perfusion pressure. The total mean survival rate of the protocol was  $80.0 \pm 7.1\%$ ; 76.9% in mI-R, 88.2% in SNJ + mI-R group in the present mI-R injury model. No differences in the occurrence of arrhythmia in SNJ + mI-R group were observed compared with that in mI-R group. This preparation is a stunned heart model [18, 19] and appropriate for our LV functional analysis because any myocardial infarctions were not observed 20 min after reperfusion (Figure 1D) as previously reported [19], although mild ischemia period persisted for 30 min in the present protocol.

#### ***Measurements of LV stroke volume and pressure volume area (PVA)***

Forty-one male Wistar rats (7-12 weeks) were used in the present experiments. The experimental protocol was shown in Figure 2. LV functions were analyzed in randomly divided 4 groups, i.e., time control, SNJ, mI-R and SNJ + mI-R group. The sample number of SNJ + mI-R were about three times higher than other groups because of the

most important group to evaluate the effect of SNJ on mI-R.

LV pressure-volume measurements at “Functional analysis” in Figure 2 were performed 60 min after coronary reperfusion. The detailed methods using conductance and pressure catheters have been described in previous reports [20-23]; LV stroke volume (SV) [= LV end-diastolic volume (EDV) – LV end-systolic volume (ESV)], end-systolic pressure at ESV ( $ESP_{ESV}$ ) and  $E_a$  (arterial effective elastance;  $ESP_{ESV} / SV^{-1}$ ) calculated from steady-state P-V loops were evaluated (Figure 3A). At midrange LVV (mLVV), end-systolic pressure ( $ESP_{mLVV}$ ) and systolic pressure-volume area ( $PVA_{mLVV}$ ; an appropriate index for evaluating cardiac total mechanical energy per beat) calculated from end-systolic pressure-volume relation (ESPVR) curve were also evaluated (Figure 3B).

The LV end-systolic P-V data on the upper left shoulder of multiple P-V loops during increasing afterload by aortic gradual occlusion were plotted and fitted by the method of least squares using the following equation:  $LVP = A\{1 - \exp[-B(LVV - V_0)]\}$ , where  $A$  and  $B$  are fitted parameters and  $V_0$  is systolic unstressed volume [20, 23-25]. Aortic gradual occlusion was performed to tighten a string occluder placed loosely around the ascending aorta until EDV slightly increased as previously reported [20, 21].

The PVA as a function of LVV was obtained by integrating the above exponential function from the extrapolated  $V_0$  along the volume axis:  $PVA = A(LVV - V_0) - A\{1 - \exp[-B(LVV - V_0)]\}/B$  [20, 23-25]. PVA is linearly related to myocardial oxygen consumption per beat [22]. Therefore,  $PVA_{mLVV}$  is a better cardiac functional index in terms of cardiac mechanoenergetics. In the present study, we calculated mLVV that was the value of [ $V_0 + (\text{maximum ESV} - \text{minimum ESV})$  on the ESPVR  $\times 1/2$ ] from all P-V loops in each group [20, 24, 25].

### **Drugs**

A synthetic, water-soluble calpain inhibitor, SNJ-1945, (SNJ: provided from Senju Pharmaceutical Co. Ltd., Kobe) was dissolved in Lactate Ringer solution at 60  $\mu\text{mol/L}$ . Other lipophilic calpain inhibitors, such as MDL28170, calpain inhibitor-3 [26] and calpain inhibitor-1 [8] have been previously dissolved in DMSO. DMSO has antioxidant properties. In the present study, we did not use DMSO to dissolve SNJ and thus our study did not include a vehicle control group. We administered SNJ solution at a dose of 0.387 mg/kg on average (60  $\mu\text{mol/L}$ , 5 ml, i.p.). 60  $\mu\text{mol/L}$  is the limit of its solubility [9]. SNJ has a  $\beta_1$  receptor stimulating action [27], but in the present study this action was not detected (Tables 2 and 3).

### ***Polyacrylamide gel electrophoresis and immunoblottings of 150-kD and 145-kD fragments of $\alpha$ -fodrin (250-kD), L-type $\text{Ca}^{2+}$ channel (LTCC) and sarcoplasmic reticulum $\text{Ca}^{2+}$ ATPase (SERCA2a)***

Membrane proteins were isolated from the LV wall of each frozen heart stored at  $-80^\circ\text{C}$  after the mechanoenergetic studies. The frozen hearts (0.1 g) were homogenized in 1ml of the STE buffer containing 0.32 mol/L sucrose, 10 mmol/L Tris-HCl, pH 7.4, 1 mmol/L EGTA, 5 mmol/L  $\text{NaN}_3$ , 10 mmol/L  $\beta$ -mercaptoethanol, 20 mmol/L leupeptin, 0.15 mmol/L pepstatin A, 0.2 mmol/L phenylmethanesulfonyl fluoride, and 50 mmol/L NaF with a Polytron homogenizer (NS-310E, Micotec Co., Ltd) and centrifuged at 1,000 x g for 10 min. The supernatants were centrifuged at 100,000 x g for 60 min at  $4^\circ\text{C}$ . The 100,000 x g pellets were cellular membrane fractions. Membrane proteins (50  $\mu\text{g/lane}$ ) were subjected to SDS-poly-acrylamide gel electrophoresis, followed by immunoblotting of 150-kD and 145-kD fragments of  $\alpha$ -fodrin (240-kD)[8, 28, 29], LTCC and SERCA2a [9]. The membranes were blocked (4% Block Ace, Dainippon

Pharmaceutical Co., Osaka) and then incubated with 2,000-fold diluted primary antibody against anti- $\alpha$ -fodrin (1:2000 dilution, Biohit, Genex), anti-LTCC antibody (1:300 dilution, Alomone Labs, Ltd., Israel) and anti-SERCA2a antibody (1:1000 dilution, Affinity Bio Reagents). The antigens were detected by the luminescence method (ECL Western blotting detection kit, Amersham) with peroxidase-linked anti-mouse IgG (1:2000 dilution) or peroxidase-linked anti-rabbit IgG (1:2000). The amounts of membrane proteins were determined to obtain the linear response of ECL-immunoblot. After immunoblotting, the film was scanned with a scanner, and the intensity of the bands was calculated by NIH image analysis. The intensity ratio of 145-, 150-kD bands versus 240-kD band ( $\alpha$ -fodrin) was expressed in an arbitrary unit and compared with that in time control (Average=1.0).

### **Statistics**

Comparison of paired and unpaired individual values was performed by paired and unpaired t-test, respectively. Multiple comparisons were performed by one-way analysis of variance (ANOVA) with post-hoc Bonferroni's test or Tukey HSD test. A value of  $p < 0.05$  was considered statistically significant. All data are expressed as the mean  $\pm$  S.D.

## **RESULTS**

All cardiac weights data comparing among different 4 groups are shown in Table 1. The smaller BWs in mI-R (7-11W), SNJ + mI-R (7-11W) groups were due to younger age than that in time control (10-12W). All mean pre and post data comparing among different 4 groups are shown in Tables 2 and 3. There were no significant differences in all hemodynamic indices of ESV, EDV, Ea and  $ESP_{ESV}$  except for post  $ESP_{ESV}$  in mI-R among time control, mI-R, SNJ + mI-R and SNJ groups (Table 2).

### ***Effects of SNJ on LV functions***

In SNJ group, each mean SV,  $ESP_{ESV}$ , Ea,  $ESP_{mLVV}$  and  $PVA_{mLVV}$  was not significantly different from each baseline data for 120 min (Tables 2 and 3), indicating no  $\beta_1$  receptor stimulating action was detected under the present experimental conditions.

### ***Effects of SNJ on LV mechanoenergetics after mI-R***

A representative set of P-V loops and ESPVRs during aortic occlusion in each group is shown in Figure 4. In mI-R group, ESPVR markedly shifted downward 60 min after mI-R (Figure 4B). In contrast, the P-V loops and ESPVR in SNJ + mI-R (Figure 4C) 30 min before and 60 min after mI-R were similar to those in time control (Figure 4A).

Mean fitting parameters, **A** and **B** of ESPVR in each group are shown in Table 3. In mI-R group, post fitting parameter **A** significantly ( $P < 0.05$ ) decreased compared with pre one. This was consistent with a marked downward-shift of ESPVR after mI-R (Figure 4B). A representative set of PVA-LVV relation curves calculated using **A** and **B** in each group is shown in Figure 5. Post mI-R PVA is decreased at any LVV in mI-R group, although the larger LVV, the larger decrease in PVA is observed (Figure 5B).

The mean absolute values of  $ESP_{mLVV}$ ,  $PVA_{mLVV}$  and  $ESP_{ESV}$  in each group are also shown in Tables 2 and 3. Post mI-R mean values of  $ESP_{mLVV}$  and  $PVA_{mLVV}$  in mI-R group were significantly ( $P < 0.05$ ) smaller than those in time control whereas those in SNJ + mI-R group were significantly ( $P < 0.05$ ) larger than those in mI-R group. Post mI-R mean values of  $ESP_{mLVV}$ ,  $PVA_{mLVV}$  and  $ESP_{ESV}$  in mI-R group were significantly ( $P < 0.05$ ) smaller than pre mI-R mean values whereas those in SNJ + mI-R group were not significantly different from pre mI-R mean values.

Mean % of baseline data in  $ESP_{mLVV}$ ,  $PVA_{mLVV}$  and  $ESP_{ESV}$  significantly ( $P < 0.05$ )

decreased compared to time control (= 100%) and that in SV moderately decreased but not significantly in mI-R group (Figure 6B). In SNJ + mI-R group, mean % of baseline data in  $ESP_{mLVV}$ ,  $PVA_{mLVV}$  and  $ESP_{ESV}$  significantly ( $P < 0.05$ ) increased from those in mI-R group to time control level (Figure 6A, C, D).

#### ***Immunoblotting of 150-kD and 145-kD fragments of $\alpha$ -fodrin (240-kD)***

Figure 7 showed immunoblottings of 240 kD  $\alpha$ -fodrin and 145- & 150-kD  $\alpha$ -fodrin proteolytic fragments in time control, mI-R and SNJ + mI-R groups. The mean amounts of 145- & 150-kD fragments in mI-R group were significantly ( $P < 0.05$ ) larger than those in time control group. The mean amounts of 145- & 150-kD fragments in SNJ + mI-R group were significantly ( $P < 0.05$ ) smaller than those in mI-R group.  $\alpha$ -fodrin mean degradation 120 min after SNJ did not increase ( $1.16 \pm 0.34$  fold;  $n=5$ ) compared with time control group ( $n=3$ ). The results indicated that  $\alpha$ -fodrin degradation after mI-R was completely prevented by SNJ treatment.

Figure 8A showed immunoblottings of LTCC in time control, mI-R and SNJ + mI-R groups. The mean amount of LTCC protein in mI-R was significantly ( $P < 0.05$ ) smaller than that in time control group. The mean amounts of LTCC protein in SNJ + mI-R group were not significantly different from those in time control and mI-R groups. The results indicated that moderate prevention of LTCC degradation after mI-R was attained by SNJ treatment.

Figure 8B showed immunoblottings of SERCA2a in time control, mI-R and SNJ + mI-R groups. The mean amount of SERCA2a protein in mI-R group was significantly ( $P < 0.05$ ) smaller than that in time control group. The mean amount of SERCA2a protein in SNJ + mI-R group increased but not significantly ( $P > 0.05$ ) and remained significantly ( $P < 0.05$ ) smaller than that in time control group, indicating partial

prevention of SERCA2a degradation after mI-R was attained by SNJ treatment.

## DISCUSSION

We have previously demonstrated that in *in vitro* rat hearts, the lipophilic calpain inhibitor, calpain inhibitor-1 attenuates  $\alpha$ -fodrin proteolysis and cardiac dysfunction due to I-R injury [8] and acute  $\text{Ca}^{2+}$  overload [7]. Recently, we also have demonstrated that a new water-soluble calpain inhibitor, SNJ exerts similar cardioprotective actions in *in vitro* rat hearts after KCl (30 mEq) cardioplegia arrest-reperfusion [9]. In the present study, we found that in *in situ* rat hearts, pretreatment of SNJ also completely prevented cardiac dysfunction and  $\alpha$ -fodrin degradation induced by mI-R.

We have previously reported that proteolysis of a cytoskeleton protein,  $\alpha$ -fodrin is found without proteolysis of ankyrin, connexin 43 and troponin I in high  $\text{Ca}^{2+}$ -infusion-induced  $\text{Ca}^{2+}$  overloaded contractile failing hearts associated with the impairment of the total  $\text{Ca}^{2+}$  handling in the excitation-contraction (E-C) coupling [7]. It seems likely that  $\alpha$ -fodrin is the most sensitive membrane protein to  $\text{Ca}^{2+}$  overload. To investigate cardiac protective effect of SNJ mediated via calpain inhibition, we focused on proteolysis of  $\alpha$ -fodrin in the present mI-R injury, because there is a close correlation between the membrane  $\alpha$ -fodrin proteolysis and the impairment of the total  $\text{Ca}^{2+}$  handling [7-9].

In addition, recent studies have revealed that calpain activation induced by I-R injury causes degradation of  $\text{Ca}^{2+}$ -handling proteins such as LTCC [30] and SERCA2a [26, 30]. Thus, we also examined the degradation of  $\text{Ca}^{2+}$ -handling proteins such as LTCC and SERCA2a in the present mI-R injury model.

It has been proposed that fodrin maintains the integrity of the plasma membranes as a

constituent of the membrane skeleton [10]. Therefore, it seems likely that the degradation of fodrin in membrane fractions would alter the properties of ion channels [12]. From the possibility that disruption of cytoskeletal proteins inactivates LTCC [13, 31], we speculate that the linkage of the LTCC to the membrane fodrin tethers the channel in place, which somehow modulates the basal activity of the channel, and a loss of the linkage may impair its regulation. Therefore, the calpain inhibitor may have protected against LV dysfunction by preserving the structural integrity of the LTCC in the cell membrane [13, 31] as in *in vitro* rat hearts after cardioplegia arrest reperfusion [9].

Although the degradation of LTCC and SERCA2a was not identified in reperfusion injury after cardioplegia cardiac arrest in *in vitro* rat hearts [9], in the present mild I-R injury in *in situ* rat hearts, the degradation of LTCC and SERCA2a was identified. SNJ attenuated the degradation of LTCC and SERCA2a, though not completely. Therefore, SNJ attenuated cardiac dysfunction possibly and partially by preventing the dysfunction of Ca<sup>2+</sup> handling proteins, such as LTCC and possibly SERCA2a. Although protein level of SERCA2a remained low, large amounts of SERCA2a protein are originally expressed in the rat myocardium and thus this level may be sufficient if some functional compensation such as activation of phosphorylation of phospholamban occurs mediated via autonomic nervous system and/or hormonal control system.

We have reported a marked  $\beta_1$  action of SNJ in the blood-perfused excised rat hearts [27]. However, in the present *in situ* heart study, no marked  $\beta_1$  action of SNJ was observed (see Tables 2 and 3). The differences between *in vitro* and *in situ* studies might have been caused by the different application methods of SNJ. In *in vitro* hearts, the direct infusion of SNJ into the coronary artery was performed, whereas in *in situ*

hearts, the indirect intraperitoneal injection of SNJ was performed.

In conclusion, a new water-soluble, which is more beneficial for clinical use, calpain inhibitor, SNJ, would be a promising tool for pharmacotherapy to exert cardioprotective actions in clinical setting. Present *in situ* mild I-R injury model hearts correspond to stunned myocardium around the necrotic focus in acute myocardial infarction in clinical setting. Upon direct percutaneous transluminal coronary angioplasty (PTCA) for acute myocardial infarction, the stunned myocardium would generate arrhythmia and myocardial contractile dysfunction. Pretreatment with SNJ upon PTCA would prevent *in vivo* heart from generating arrhythmia and myocardial dysfunction.

#### *Limitation of the study*

The measurement of the expression levels of other  $\text{Ca}^{2+}$  handling proteins, such as  $\text{Na}^+$ - $\text{Ca}^{2+}$ -exchanger, phospholamban and ryanodine receptor would be expected for better understanding of the function of  $\text{Ca}^{2+}$  handling in E-C coupling in the future work.

#### **Acknowledgments**

This work was supported in part by grants-in-aid NO. 22790216 for Scientific Research from the Ministry of Education, Culture, Sports, Science and Technology of Japan. We also thank Senju Pharmaceutical Co. Ltd., Kobe for providing us SNJ-1945.

#### **Statement of conflicts of interest**

None

#### **Author Contributions:**

Miyako Takaki designed and supervised the present study. Daisuke Takeshita, Midori

Tanaka, Shinichi Mitsuyama, Guo-Xing Zhang, Koji Obata, Haruo Ito and Miyako Takaki conducted experiments and obtained the data. Yoshiro Yoshikawa and Shigeki Taniguchi supervised the present study. Daisuke Takeshita and Miyako Takaki performed the data analysis and drafted the manuscript.

## References

1. Hagihara H, Yoshikawa Y, Ohga Y, Takenaka C, Murata K, Taniguchi S, Takaki M (2005)  $\text{Na}^+/\text{Ca}^{2+}$  exchange inhibition protects the rat heart from ischemic-reperfusion injury by blocking energy-wasting processes. *Am J Physiol Heart Circ Physiol* 288: H1699-H1707
2. Karmazyn M, Gan XT, Humphreys RA, Yoshida H, Kusumoto K (1999) The myocardial  $\text{Na}^+/\text{H}^+$  exchange structure, regulation, and its role in heart disease. *Circ Res* 85: 777-786
3. Schäfer C, Ladilov Y, Inserte J, Schäfer M, Haffner S, Garcia-Dorado D, Piper HM (2001) Role of the reverse mode of the  $\text{Na}^+/\text{Ca}^{2+}$  exchanger in reoxygenation-induced cardiomyocyte injury. *Cardiovasc Res* 51: 241-250
4. Tani M, Neely JR (1989) Role of intracellular  $\text{Na}^+$  in  $\text{Ca}^{2+}$  overload and depressed recovery of ventricular function of reperfused ischemic rat hearts. Possible involvement of  $\text{H}^+-\text{Na}^+$  and  $\text{Na}^+-\text{Ca}^{2+}$  exchange. *Circ Res* 65: 1045-1056
5. Kobayashi S, Yoshikawa Y, Sakata S, Takenaka C, Hagihara H, Ohga Y, Abe T, Taniguchi S, Takaki M (2004) Left ventricular mechanoenergetics after hyperpolarized cardioplegic arrest by nicorandil and after depolarized cardioplegic arrest by KCl. *Am J Physiol Heart Circ Physiol* 287: H1072-1080
6. Opie LH (1998) Chap.19 Myocardial reperfusion. In: *The Heart. Physiology, from Cell to Circulation*. Lippincott-Raven Press: Philadelphia, New York, PP563-588
7. Tsuji T, Ohga Y, Yoshikawa Y, Sakata S, Abe T, Tabayashi N, Kobayashi S, Kitamura S, Taniguchi S, Suga H, Takaki M (2001) Rat cardiac contractile dysfunction induced

- by  $\text{Ca}^{2+}$  overload: Possible link to the proteolysis of fodrin. *Am J Physiol Heart Circ Physiol* 281: H1286-H1294
8. Yoshikawa Y, Hagihara H, Ohga Y, Nakajima-Takenaka C, Murata K, Taniguchi S, Takaki M (2005) Calpain inhibitor-1 protects the rat heart from ischemic-reperfusion injury: analysis by mechanical work and energetics. *Am J Physiol Heart Circ Physiol* 288: H1690-H1698
  9. Yoshikawa Y, Zhang G-X, Obata K, Ohga Y, Matsuyoshi H, Taniguchi S, Takaki M (2010) Cardioprotective effects of a novel calpain inhibitor, SNJ-1945 for reperfusion injury after cardioplegic cardiac arrest. *Am J Physiol Heart Circ Physiol* 298: H643-H651
  10. Bennett V (1990) Spectrin-based membrane skeleton: a multipotential adaptor between plasma membrane and cytoplasm. *Physiol Rev* 70: 1029-1065
  11. Lazarides E, Nelson WJ (1983) Erythrocyte and brain forms of spectrin in cerebellum: distinct membrane-cytoskeletal domains in neurons. *Science* 220: 1295-1296
  12. Yoshida K, Inui M, Harada K, Saido TC, Sorimachi Y, Ishihara T, Kawashima S, Sobue K (1995) Reperfusion of rat heart after brief ischemia induces proteolysis of caldesmon (nonerythroid spectrin or fodrin) by calpain. *Circ Res* 77: 603-610
  13. Galli A, DeFelice LJ (1994) Inactivation of L-type Ca channels in embryonic chick ventricle cells: dependence on the cytoskeletal agents colchicine and taxol. *Biophys J* 67: 2296-2304
  14. Oka T, Walkup RD, Tamada Y, Nakajima E, Tochigi A, Shearer TR, Azuma M (2006) Amelioration of retinal degeneration and proteolysis in acute ocular

- hypertensive rats by calpain inhibitor ((1S)-1((((1S)-1-benzyl-3-cyclopropylamino-2,3-di-oxo-propyl) amino) carbonyl)-3-methylbutyl) carbamic acid 5-methoxy-3-oxapentyl ester. *Neuroscience* 141: 2139-2145
15. Shirasaki Y, Yamaguchi M, Miyashita H (2006) Retinal penetration of calpain inhibitors in rats after oral administration. *J Ocul Pharmacol* 22: 417-424.
  16. Koumura A, Nonaka Y, Hyakkoku K, Oka T, Shimazawa M, Hozumi I, Inuzuka T, Hara H (2008) A novel calpain inhibitor, ((1S)-1((((1S)-1-benzyl-3-cyclopropyl-amino-2,3-di-oxopropyl) amino) carbonyl)-3-methylbutyl) carbamic acid 5-methoxy-3-oxapentyl ester, protects neuronal cells from cerebral ischemia-induced damage in mice. *Neuroscience* 157: 309-318
  17. Ito H, Takaki M, Yamaguchi H, Tachibana H, Suga H (1996) Left ventricular volumetric conductance catheter for rats. *Am J Physiol* 270: H1509-H1514
  18. Braunwald E, Kloner RA (1982) The stunned myocardium: prolonged, postischemic ventricular dysfunction. *Circulation* 66: 1146-1149
  19. Hamilton KL, Powers SK, Sugiura T, Kim S, Lennon S, Tumer N, Mehta JL (2001) Short-term exercise training can improve myocardial tolerance to I/R without elevation in heat shock proteins. *Am J Physiol Heart Circ Physiol* 281: H1346-H1352
  20. Kitagawa Y, Yamashita D, Ito H, Takaki M (2004) Reversible effects of isoproterenol-induced hypertrophy on in situ left ventricular function in rat hearts. *Am J Physiol Heart Circ Physiol* 28: H277-H285
  21. Tachibana H, Takaki M, Lee S, Ito H, Yamaguchi H, Suga H (1997) New mechanoenergetic evaluation of left ventricular contractility in in situ rat hearts. *Am J Physiol Heart Circ Physiol* 272: H2671-H2678

22. Takaki M (2004) Left ventricular mechanoenergetics in small animals. *Jpn J Physiol* 54: 175-207
23. Takeshita D, Shimizu J, Kitagawa Y, Yamashita D, Tohne K, Nakajima-Takenaka C, Ito H, Takaki M (2008) Isoproterenol-induced hypertrophied rat hearts: does short-term treatment correspond to long-term treatment? *J Physiol Sci* 58: 179-188
24. Kuzumoto N, Kitagawa Y, Uemura K, Ueyama T, Yoshida K, Furuya H, Takaki M (2004) A brief regional ischemic-reperfusion enhances propofol-induced depression in left ventricular function of in situ rat hearts. *Anesthesiology* 101: 879-887
25. Nakahashi K, Kitagawa Y, Ito H, Kuzumoto N, Furuya H, Takaki M (2005) Positive inotropic effect of nicorandil in in situ adult rats. *J Anesth* 19: 45-53
26. French JP, Quindry JC, Falk DJ, Staib JL, Lee Y, Wang KKW, Powers SK (2006) Ischemia-reperfusion-induced calpain activation and SERCA2a degradation are attenuated by exercise training and calpain inhibition. *Am J Physiol Heart Circ Physiol* 290: H128-H136
27. Yoshikawa Y, Zhang G-X, Obata K, Matsuyoshi H, Asada K, Taniguchi S, Takaki M (2010) A cardioprotective agent of a novel calpain inhibitor, SNJ-1945 exerts  $\beta_1$ -actions on left ventricular mechanical work and energetics. *Am J Physiol Heart Circ Physiol* 299: H396-H401
28. Towbin H, Staehelin T, Gordon J (1979) Electrophoretic transfer of proteins from polyacrylamide gels to nitrocellulose sheets: procedure and some applications. *Proc Natl Acad Sci USA* 76: 4350-4354
29. Yoshida K, Yamasaki Y, Kawashima S (1993) Calpain activity alters rat myocardial subfractions after ischemia and reperfusion. *Biochim Biophys Acta* 1182: 215-220

30. French JP, Hamilton KL, Quindry JC, Lee Y, Upchurch PA, Powers SK (2008) Exercise-induced protection against myocardial apoptosis and necrosis: MnSOD, calcium-handling proteins, and calpain. *The FASEB Journal* 22: 2862-2871
31. Nakamura M, Sunagawa M, Kosugi T, Sperelakis N (2000) Actin filament disruption inhibits L-type  $\text{Ca}^{2+}$  channel current in cultured vascular smooth muscle cells. *Am J Physiol Cell Physiol* 279: C480-C487

### Legend for Figures

**Figure 1.** Mild ischemic-reperfusion (mI-R) heart preparation. a: Coronary gradual and partial occlusion was performed in 10 seconds by ligation of proximal left anterior descending artery and attached 1-mm diameter soft tube (as buffer) using a bulldog clamp at the knot of 4-0 polypropylene suture under monitoring LV pressure-volume (P-V) loop. b: Typical left ventricular (LV) pressure-volume loops during gradual and partial coronary occlusion to make mild ischemic-reperfusion heart preparations. c: A typical macrograph of the preparation of time control. d: A typical LV macrograph of the mI-R preparations obtained 20 min after mI-R. No myocardial infarction was observed. e: A typical macrograph of the preparation of acute myocardial infarction (MI) obtained 20 min after severe I-R. The infarct tissue was indicated by white dotted boundary. It appeared white even by naked eyes. The non-injured tissue was indicated by an arrow outside the infarct tissue.

**Figure 2.** Experimental protocols of the four group. 1. Time control group (n=5); 2. SNJ group (n=5); 3. mI-R group (n=6); 4. SNJ + mI-R group (n=15).

**Figure 3.** Evaluation of left ventricular (LV) function by end-systolic pressure-volume relation (ESPVR) using pressure-volume (P-V) measurements. Enveloping curve of end-systolic pressure at end-systolic volume ( $ESP_{ESV}$ ) data of several P-V loops during aortic gradual occlusion (gradually increasing afterload) corresponds to ESPVR.

SV, stroke volume; ESV, end-systolic volume; EDV, end-diastolic volume;  $E_a$ , effective arterial elastance.  $mLVV$ , midrange LV volume;  $V_0$ , LV volume intercept;  $ESP_{mLVV}$ , end-systolic pressure at  $mLVV$ ;  $PVA_{mLVV}$ , systolic pressure-volume area at  $mLVV$ .

**Figure 4.** A representative set of P-V loops and ESPVRs during aortic occlusion in each group. Each onset and offset P-V loop and ESPVRs at baseline and 120 min after baseline are indicated by gray solid and black dotted lines in time control group (a), respectively. Each onset and offset P-V loop and ESPVRs 30 min before and 60 min after mI-R are indicated by gray solid and black dotted lines in mI-R (b) and SNJ + mI-R groups (c), respectively. Solid arrow in (b) indicates downward shift of ESPVR.  $V_0$ : LV volume intercept.

**Figure 5.** PVA-LVV relationship curves in time control (a), mI-R (b) and SNJ + mI-R groups (c), respectively. PVA-LVV relationship curves 30 min before and 60 min after mI-R are indicated by gray solid and black dotted lines, respectively. Solid arrow in b indicates downward shift of PVA-LVV relation curve.  $V_0$ : LV volume intercept.

**Figure 6.** Mean percent of baseline data in  $ESP_{mLVV}$  (a), SV (b),  $PVA_{mLVV}$  (c) and  $ESP_{ESV}$  (d) 60 min after mI-R in each group. Data show the mean with SD. \*,  $P < 0.05$  versus time control. #,  $P < 0.05$  versus mI-R.

**Figure 7.** Ratio of 150-, 145-kD proteolytic fragments by calpain to 240-kD intact  $\alpha$ -fodrin in the time control, mI-R and SNJ + mI-R groups. Upper panel: each representative band in the time control, mI-R and SNJ + mI-R groups. All bands were obtained from the same SDS-polyacrylamide gel. Lower panel: Mean fold change of 150-, 145-kD fragments to 240-kD  $\alpha$ -fodrin compared to mean value (=1.0) in the time control (n=9) among the mI-R (n=9) and SNJ + mI-R (n=5) groups. Data show the

mean with SD. \*,  $P < 0.05$  versus time control. #,  $P < 0.05$  versus mI-R.  
Immunoblotting of 150- and 145-kD fragments of  $\alpha$ -fodrin (240-kD)

**Figure 8.** Comparison of LTCC protein levels (a) and SERCA2a (b) among the time control, mI-R and SNJ + mI-R groups. Upper panels: each representative band in the time control, mI-R and SNJ + mI-R groups. All bands of LTCC (a) and SERCA2a (b) were obtained from the same SDS-polyacrylamide gels, respectively. Lower panels: Mean fold changes of LTCC (a) and SERCA2a (b) compared to the mean value (=1.0) in the time control (n=6) group among the mI-R (n=6) and SNJ + mI-R (n=6) groups. Data show the mean with SD. \*,  $P < 0.05$  versus time control.

Table 1. Comparison of cardiac weights among Time control, mI-R, SNJ + mI-R and SNJ groups

	Time control (n=5)	mI-R (n=6)	SNJ + mI-R (n=15)	SNJ (n=5)
BW (g)	436 ± 30.5	319 ± 47.2*	353 ± 60.1*	388 ± 68.7
LVW (g)	0.729 ± 0.062	0.666 ± 0.078	0.676 ± 0.064	0.711 ± 0.174
RVW (g)	0.185 ± 0.021	0.164 ± 0.015	0.166 ± 0.031	0.152 ± 0.053
HWBW <sup>-1</sup>	2.10 ± 0.068	2.63 ± 0.303*	2.43 ± 0.347	2.20 ± 0.172
LVWBW <sup>-1</sup>	1.67 ± 0.096	2.11 ± 0.248*	1.95 ± 0.276	1.82 ± 0.138
RVWBW <sup>-1</sup>	0.426 ± 0.051	0.523 ± 0.082	0.481 ± 0.109	0.383 ± 0.063

BW: body weight; LVW: left ventricle weight; RVW: right ventricle weight; HW: heart weight; HW BW<sup>-1</sup>: the ratio of HW to BW; LVW BW<sup>-1</sup>: the ratio of LVW to BW; RVW BW<sup>-1</sup>: the ratio of RVW to BW; Values are mean ± SD. \*P < 0.05 vs. Time control. The sample number of SNJ + mI-R were about three times higher than other groups because of the most important group to evaluate the effect of SNJ on mI-R.

Table 2. Hemodynamics in Time control, mI-R, SNJ + mI-R and SNJ groups

		Time control (n=5)	mI-R (n=6)	SNJ + mI-R (n=15)	SNJ (n=5)
ESV (ml)	Pre	0.062 ± 0.019	0.053 ± 0.024	0.070 ± 0.022	0.078 ± 0.012
	Post	0.083 ± 0.042	0.117 ± 0.042	0.116 ± 0.037	0.086 ± 0.017
EDV (ml)	Pre	0.161 ± 0.040	0.158 ± 0.039	0.165 ± 0.027	0.170 ± 0.025
	Post	0.177 ± 0.059	0.209 ± 0.052	0.206 ± 0.041	0.179 ± 0.033
SV (ml)	Pre	0.098 ± 0.022	0.105 ± 0.019	0.095 ± 0.019	0.092 ± 0.019
	Post	0.094 ± 0.021	0.091 ± 0.026	0.090 ± 0.016	0.094 ± 0.016
ESV (ml g <sup>-1</sup> )	Pre	0.085 ± 0.021	0.081 ± 0.038	0.104 ± 0.036	0.116 ± 0.037
	Post	0.113 ± 0.054	0.180 ± 0.071	0.172 ± 0.057	0.125 ± 0.034
EDV (ml g <sup>-1</sup> )	Pre	0.219 ± 0.042	0.238 ± 0.055	0.245 ± 0.039	0.253 ± 0.071
	Post	0.241 ± 0.072	0.318 ± 0.089	0.306 ± 0.061	0.261 ± 0.069
SV (ml g <sup>-1</sup> )	Pre	0.134 ± 0.023	0.157 ± 0.022	0.140 ± 0.023	0.136 ± 0.039
	Post	0.128 ± 0.025	0.138 ± 0.039	0.134 ± 0.024	0.136 ± 0.035
ESP <sub>ESV</sub> (mmHg)	Pre	89.7 ± 10.3	90.4 ± 11.3	86.9 ± 9.5	86.5 ± 6.2
	Post	88.5 ± 6.4	71.4 ± 10.9*	85.3 ± 12.1	86.9 ± 4.2
Ea (mmHg ml <sup>-1</sup> g <sup>-1</sup> )	Pre	681 ± 116	584 ± 105	642 ± 161	686 ± 237
	Post	712 ± 149	551 ± 176	651 ± 132	669 ± 159
HR (beats min <sup>-1</sup> )	Pre	330 ± 21	354 ± 29	369 ± 33	360 ± 30
	Post	316 ± 31	342 ± 29	336 ± 38	348 ± 39

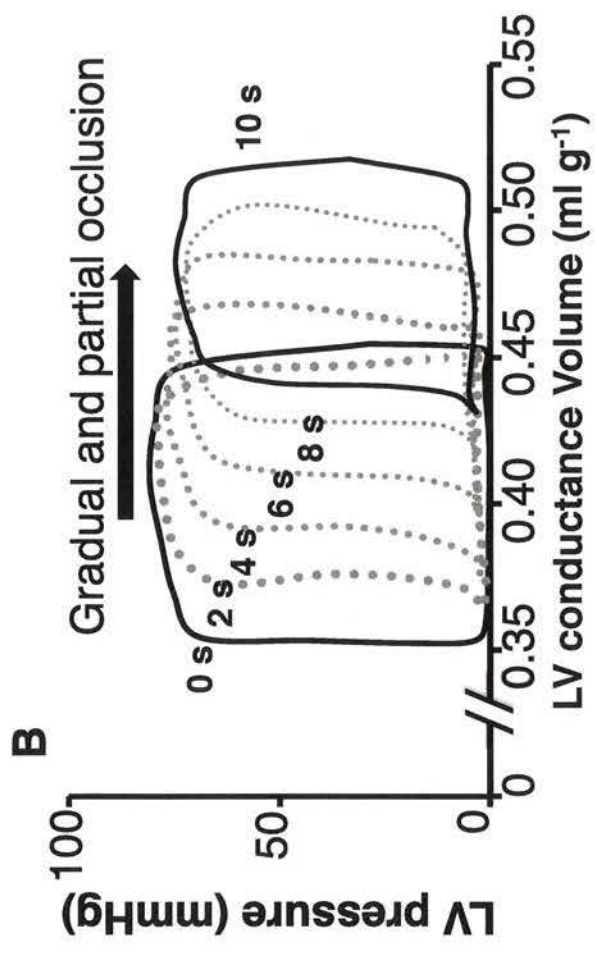
Pre: baseline data; Post: 120 min after baseline data; mI-R: mild ischemic-reperfusion; ESV (ml):

absolute end-systolic volume; EDV (ml): absolute end-diastolic volume; SV (ml): absolute stroke volume; ESV, EDV and SV ( $\text{ml g}^{-1}$ ): each volume normalized by LVW;  $\text{ESP}_{\text{ESV}}$ : end-systolic pressure;  $E_a$ : effective arterial elastance ( $= \text{ESP}_{\text{ESV}} \text{SV}^{-1}$ ); HR: heart rate. To compare volume data among different size of hearts, normalization by LVW is dispensable. Values are mean  $\pm$  SD. \* $P < 0.05$  vs. Pre. The sample number of SNJ + mI-R were about three times higher than other groups because of the most important group to evaluate the effect of SNJ on mI-R.

Table 3. Variables of left ventricular mechanics in Time control, mI-R, SNJ + mI-R and SNJ groups

		Time control (n=5)	mI-R (n=6)	SNJ + mI-R (n=15)	SNJ (n=5)
ESPVR					
<i>A</i> (mmHg)	Pre	151 ± 25.7	153 ± 22.5	144 ± 25.9	130 ± 4.3
	Post	126 ± 24.4	101 ± 23.6 <sup>\$</sup>	135 ± 33.7	131 ± 11.4
<i>B</i> (ml <sup>-1</sup> )	Pre	36.4 ± 14.5	21.9 ± 8.5	22.7 ± 13.5	21.9 ± 6.8
	Post	53.2 ± 17.7	28.4 ± 16.8*	24.5 ± 13.3*	26.3 ± 6.9*
<i>V</i> <sub>0</sub> (ml g <sup>-1</sup> )		0.058 ± 0.012	0.041 ± 0.037	0.066 ± 0.042	0.077 ± 0.036
mLVV (ml g <sup>-1</sup> )		0.137 ± 0.012	0.141 ± 0.037	0.167 ± 0.042	0.178 ± 0.036
ESPmLVV (mmHg)	Pre	123.3 ± 9.6	120.1 ± 11.6	115.5 ± 16.4	112.5 ± 14.6
	Post	116.2 ± 12.6	85.8 ± 13.7* <sup>\$</sup>	112.1 ± 20.9 <sup>#</sup>	117.4 ± 8.6 <sup>#</sup>
PVA <sub>mLVV</sub> (mmHg ml beat <sup>-1</sup> g <sup>-1</sup> )	Pre	7.81 ± 2.50	8.48 ± 1.47	7.88 ± 1.88	7.73 ± 1.45
	Post	7.46 ± 0.87	5.06 ± 1.06* <sup>\$</sup>	7.43 ± 1.61 <sup>#</sup>	7.56 ± 0.47 <sup>#</sup>

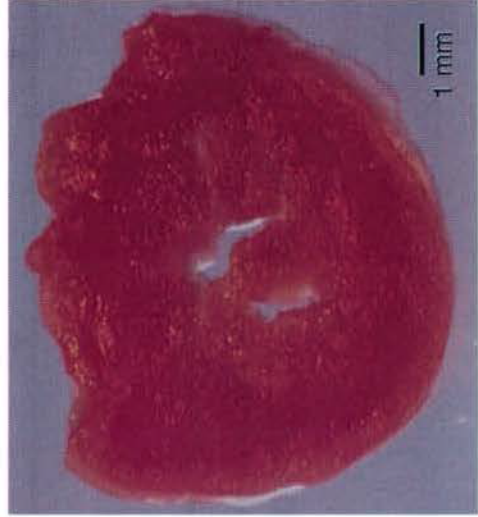
Pre: baseline data; Post: 120 min after baseline data; End-systolic pressure-volume relation (ESPVR) curve was obtained by the formula  $LVP = A\{1 - \exp[-B(LVV - V_0)]\}$ , where *A* and *B* are fitted parameters and *V*<sub>0</sub> is LV volume intercept (= systolic unstressed volume) (11, 15, 17, 25). mLVV: midrange LV volume. ESP<sub>mLVV</sub>: end-systolic pressure at mLVV. Systolic pressure-volume area (PVA) was obtained by the formula  $PVA = A(LVV - V_0) - A\{1 - \exp[-B(LVV - V_0)]\}/B$  (11, 15, 17, 25). PVA<sub>mLVV</sub>: PVA at mLVV. Values are mean ± SD. \*P < 0.05 vs. Time control. <sup>#</sup>P < 0.05 vs. mI-R. <sup>\$</sup>P < 0.05 vs. Pre. The sample number of SNJ + mI-R were about three times higher than other groups because of the most important group to evaluate the effect of SNJ on mI-R.



**C Time control**



**D ml-R**



**E MI** — Infarcted tissue

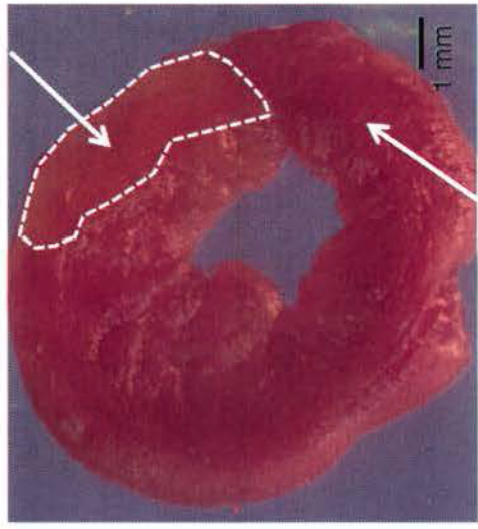


Fig. 1

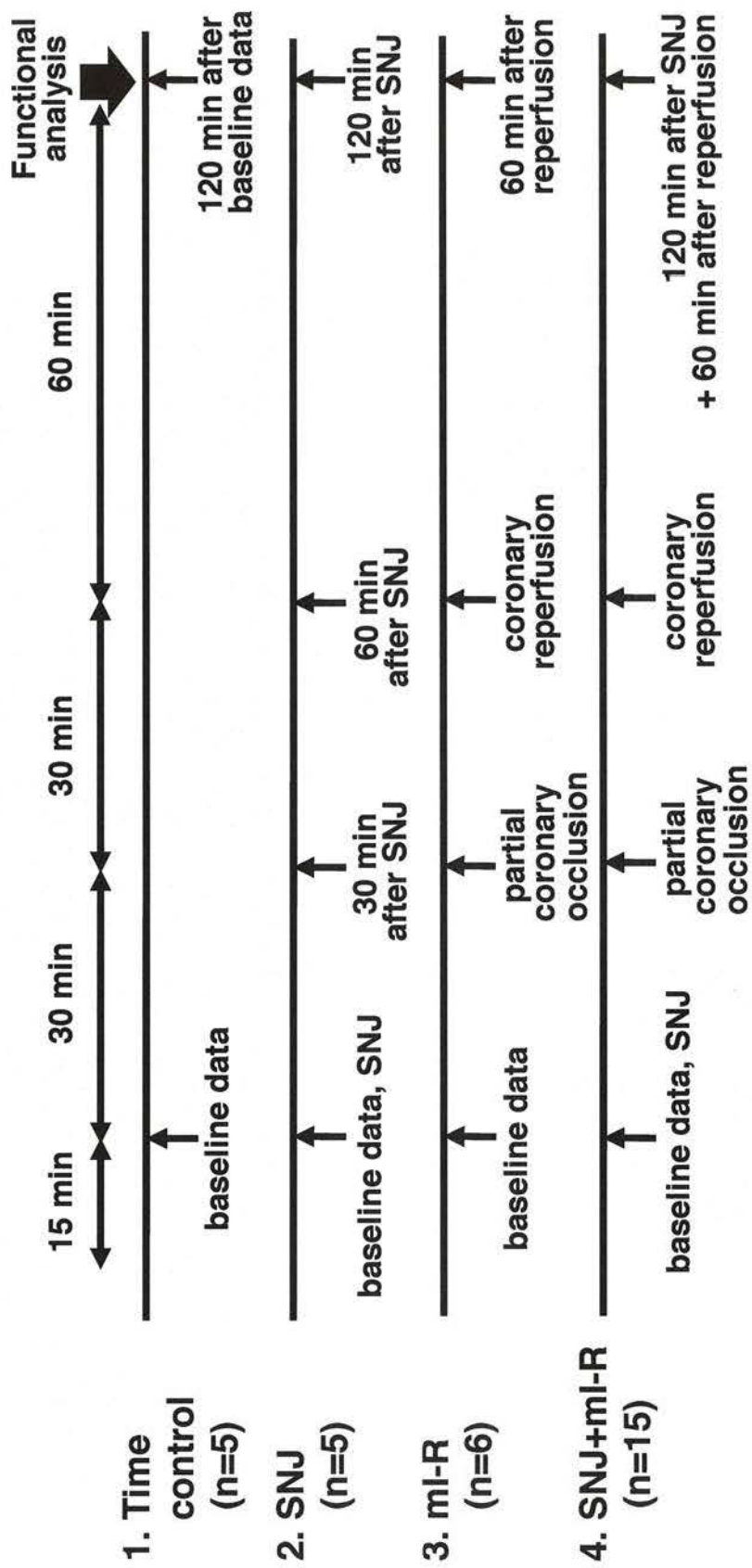


Fig. 2

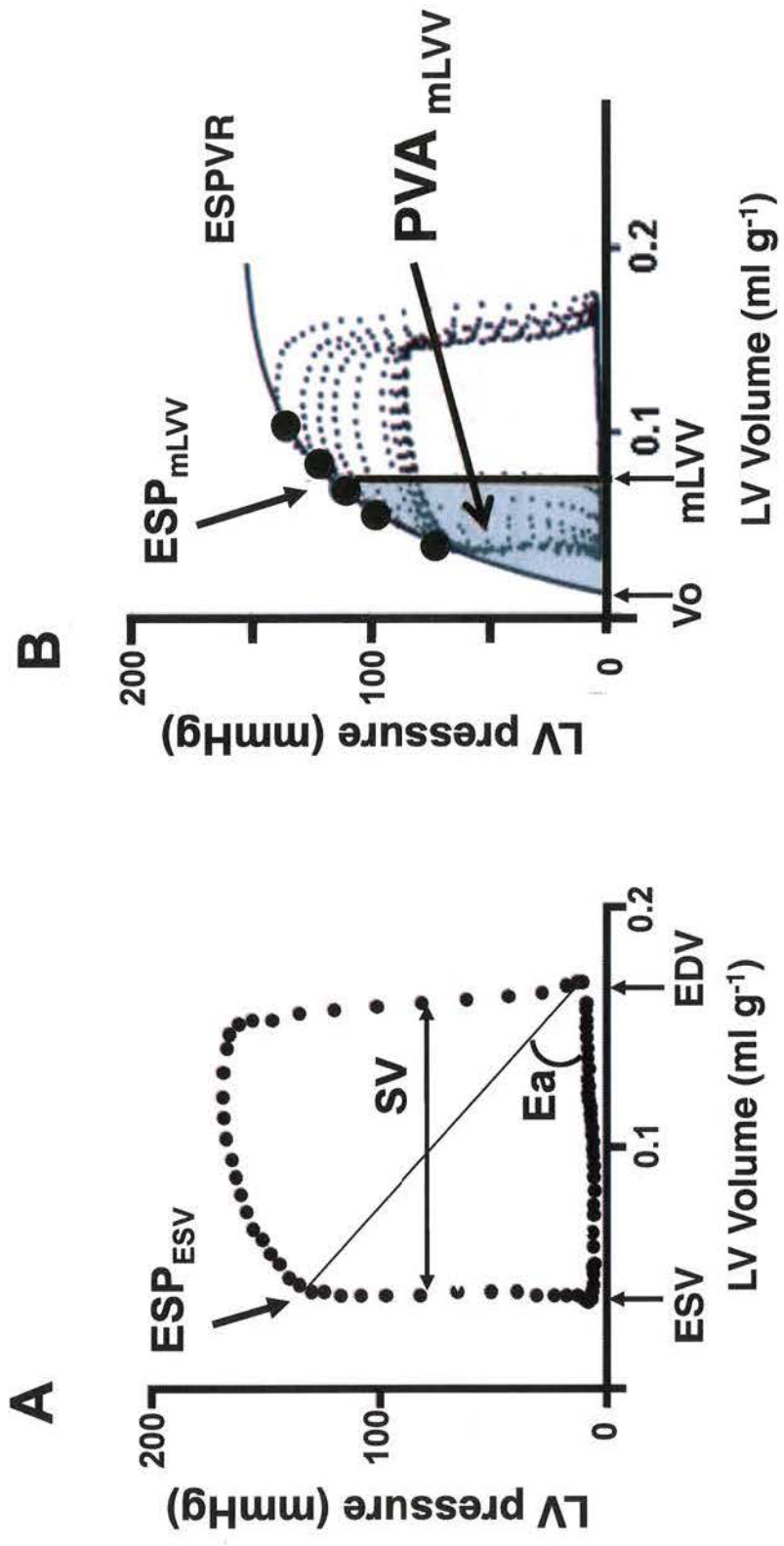


Fig. 3

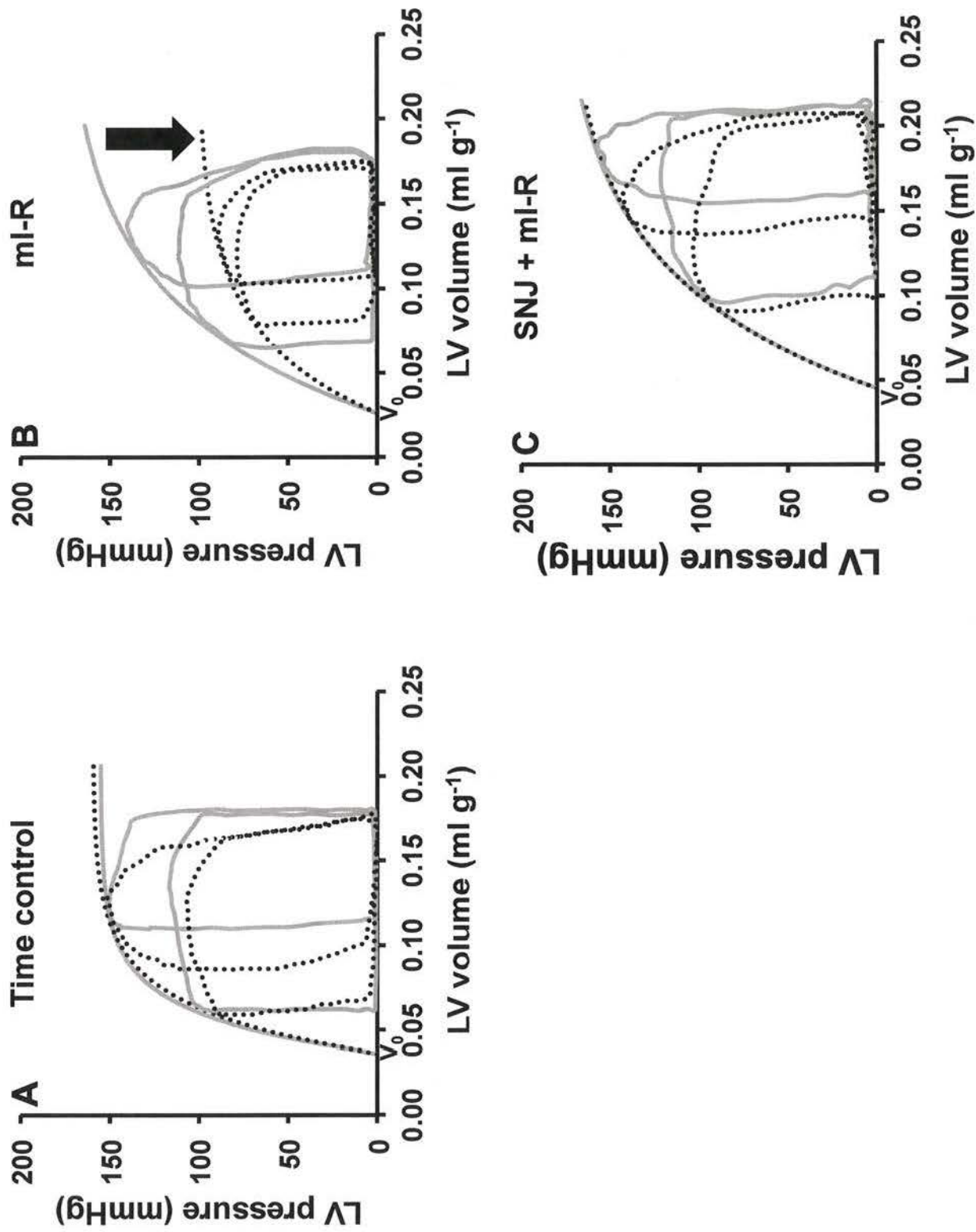


Fig. 4

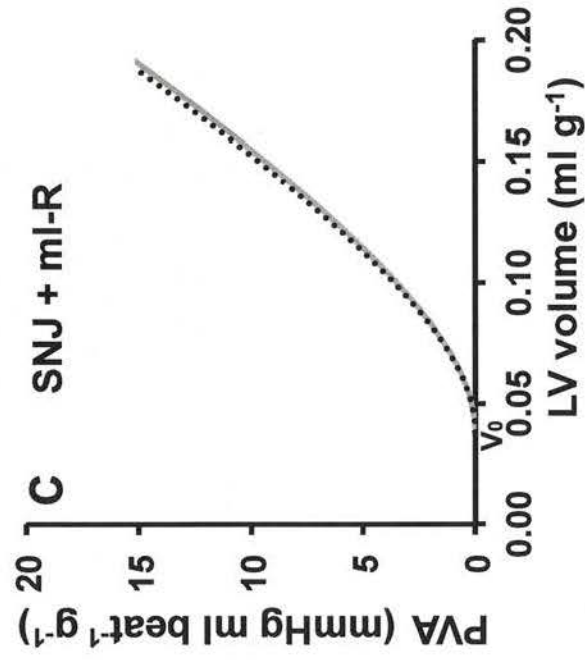
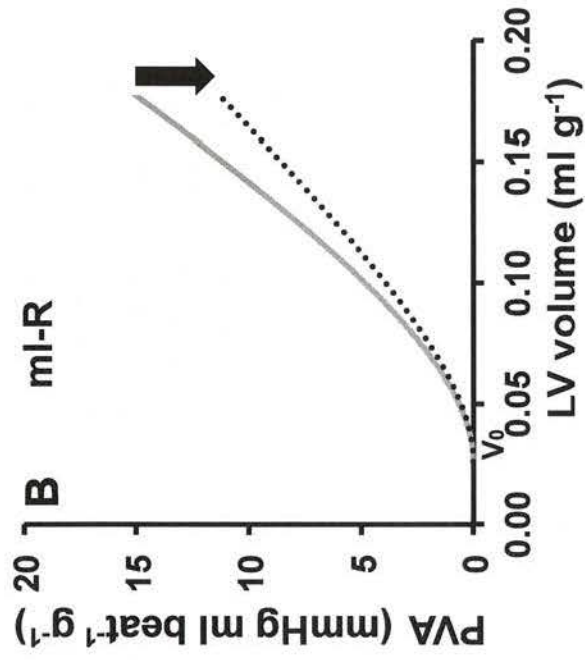
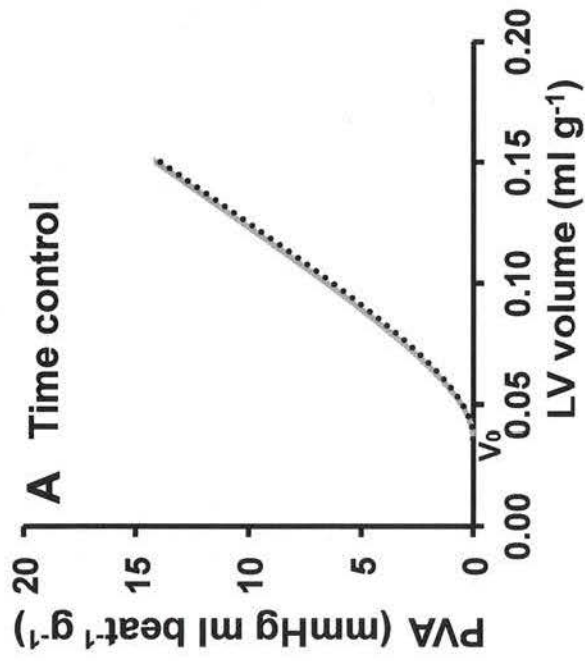


Fig. 5

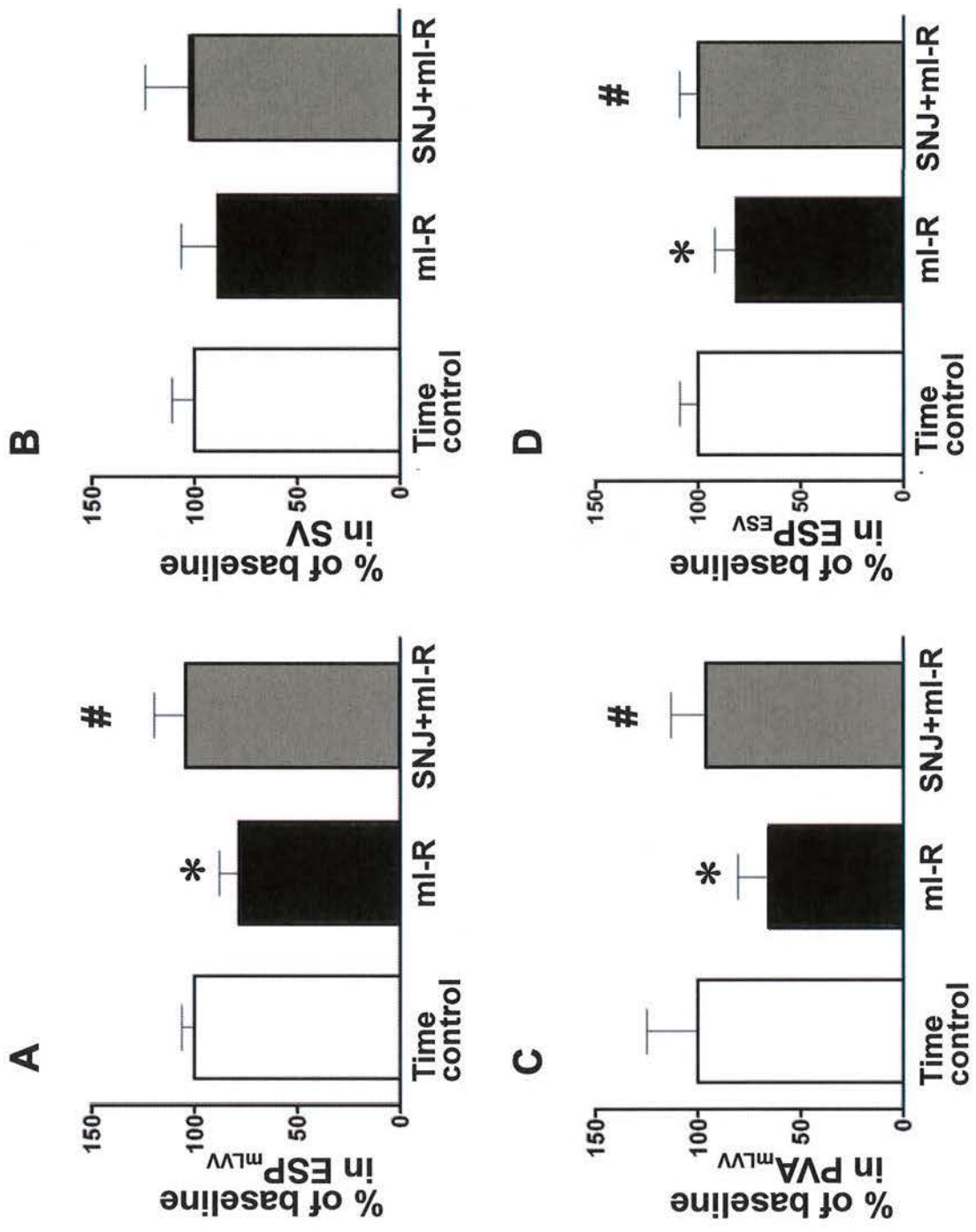


Fig. 6

**α-Fodrin**

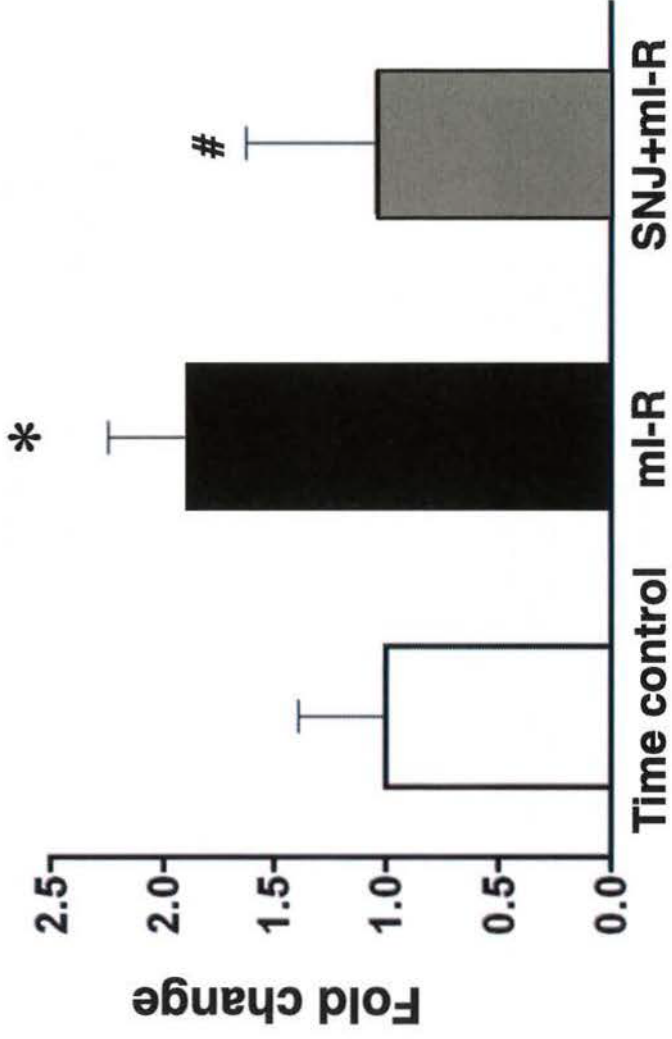
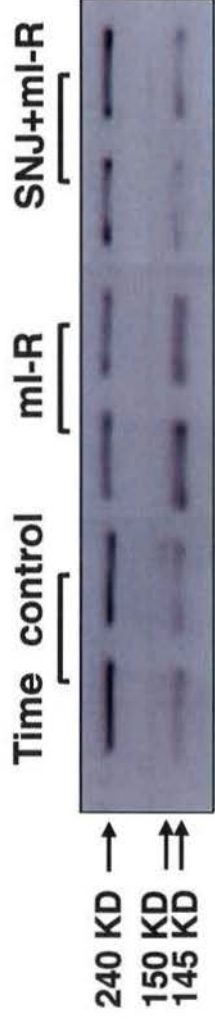


Fig. 7

LTCC

**A**

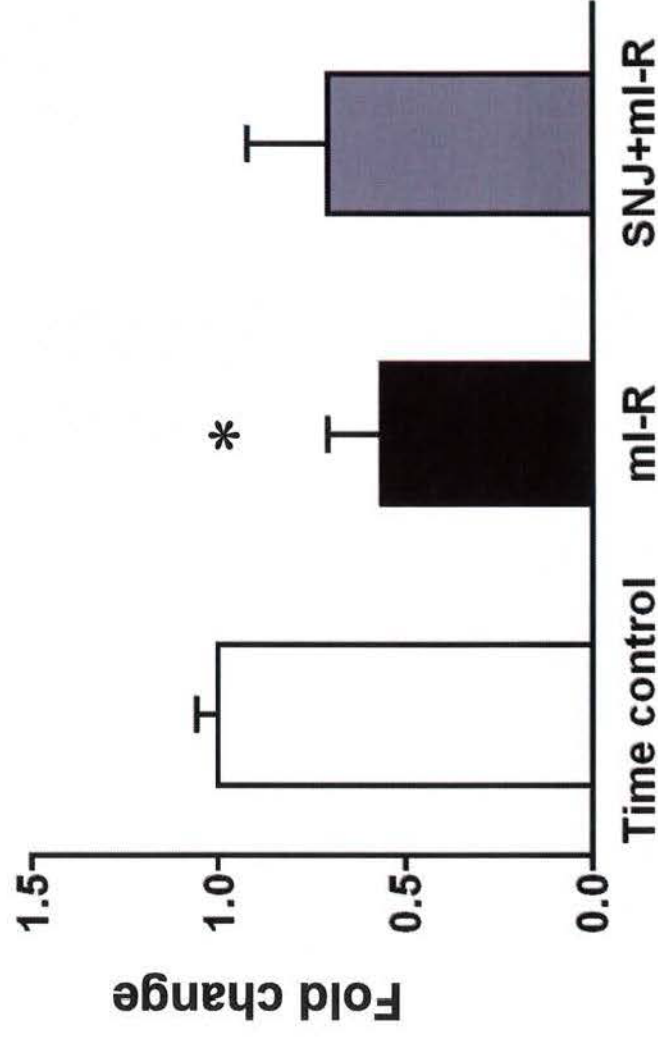
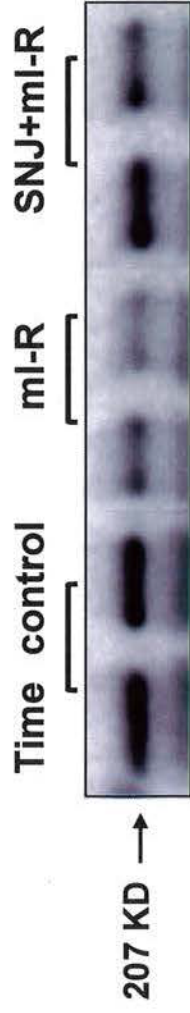


Fig. 8A

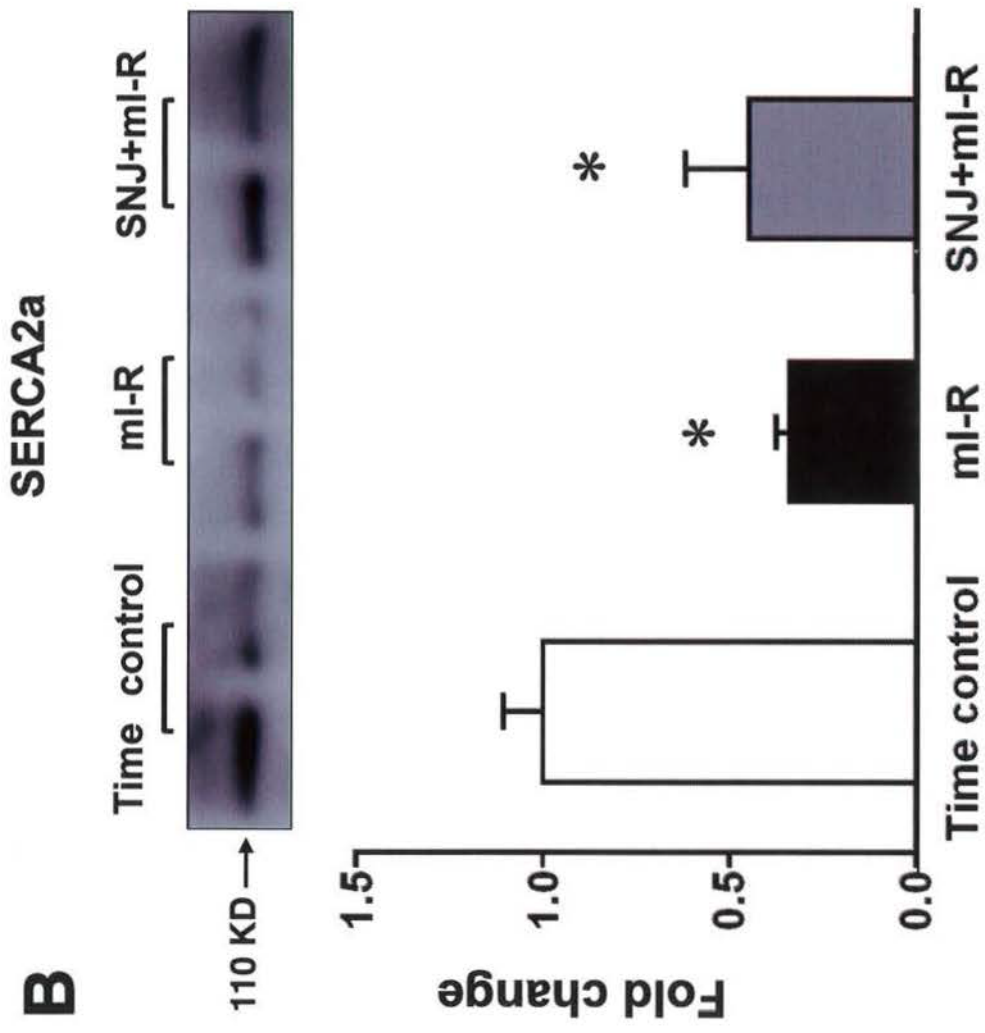


Fig. 8B